metals

MDPI

Article

Mechanical Properties of ARMCO® Iron after Large and Severe Plastic Deformation—Application Potential for Precursors to Ultrafine Grained Microstructures

Enrico Bruder

Physical Metallurgy Division, TU Darmstadt, Alarich-Weiss-Str. 2, 64287 Darmstadt, Germany; e.bruder@phm.tu-darmstadt.de; Tel.: +49-6151-1620556

Received: 22 December 2017; Accepted: 14 March 2018; Published: 17 March 2018

Abstract: Ultrafine grained (UFG) metals processed by severe plastic deformation (SPD) are well known for their outstanding mechanical properties, yet, current applications are very limited mostly due to the elaborate processing. The present work investigates the microstructures and mechanical properties of precursors to UFG microstructures that evolve at strains below the levels required for UFG microstructures, which implies less processing effort. ARMCO® iron is subjected to a single pass of equal channel angular pressing (ECAP), cold rolling, as well as a combination of both processes and compared to strain–free samples and a UFG reference condition subjected to five ECAP passes. All conditions are characterized regarding their microstructures and mechanical properties using electron backscatter diffraction, tensile tests, and rotating bending fatigue test. The precursor states show intermediate properties in between those of the strain-free and the UFG reference condition. Compared to the processing effort, the difference in properties between precursors and UFG reference is relatively small. Especially a combination of a single ECAP pass followed by cold rolling is a good compromise in terms of processing effort and mechanical properties with an endurance limit being less than 10% lower as compared to the UFG reference condition.

Keywords: fatigue; severe plastic deformation; UFG microstructures; ECAP; rolling

1. Introduction

Grain refinement of metals and alloys as a method to increase their strength is being used systematically since several decades. Severe plastic deformation (SPD) techniques—such as equal-channel angular pressing (ECAP) [1], high pressure torsion [2], or accumulative roll bonding [3]—have proven to be capable of refining microstructures down to the submicron regime [1–4], which is usually beyond the limit of conventional thermomechanical processing. Most SPD processes are derived from metal forming processes such as extrusion, rolling, or swaging. In contrast to their related forming processes, SPD processes are characterized by an invariance of the sample geometry [4], which facilitates the accumulation of severe plastic strains. The severe straining results in a grain fragmentation, i.e., dislocations forming low angle boundaries (LAGBs), which gradually transform into high angle boundaries (HAGBs) upon increasing strain [5]. The defect accumulation that leads to microstructural refinement and a corresponding increase in strength during SPD processing, but also cold working in general, is not proportional to the imposed strain. The rate of defect storage and structural refinement decreases significantly with increasing strain due to dynamic recovery effects, hence, the change in mechanical properties after the first ECAP pass is typically much stronger than for subsequent passes [1,5–9]. With regard to the elaborate processing required for the generation of an ultrafine grained (UFG) microstructure with a majority of HAGBs and submicron grain

size, one might raise the question as to whether the precursor states can provide a better compromise in terms of price-performance ratio. In fact, the use of SPD processes in general could be questioned when considering that precursors to UFG microstructures can typically be generated more economically by conventional cold forming processes.

While there is a lot of data on the evolution of hardness or tensile strength as a function of strain [6–11], this is less so for fatigue properties, even though they are technologically often more relevant than properties under monotonic loading. It has been argued that the improved fatigue strength of UFG metals is attributed to the large fraction of HAGBs, which are more stable under cyclic loading than LAGBs [12–14]. While there is evidence for a correlation between cyclic softening and LAGB fraction at high strain amplitudes (low cycle fatigue regime) [13,14], the situation is less clear for lower strain amplitudes (high cycle fatigue regime). There is usually no significant cyclic softening (or grain coarsening) observed in this regime under stress controlled tests, even though strain controlled high cycle fatigue testing can result in a softening for UFG Cu, as has been shown by Kunz et al. [15,16]. Irrespective of the presence or absence of cyclic softening, the formation of shear bands, which is accompanied by a local coarsening of the microstructure, is generally the main mechanisms leading to fatigue cracks [12,16,17]. Consequently, precursors to UFG microstructures, which show a large fraction of LAGBs, appear to be no promising candidates for applications at high strain amplitudes and this might hold for applications with lower strain amplitudes, too. However, there are also indications that the HAGB fraction is not as decisive with respect to fatigue strength in the high cycle fatigue regime. An overview by Estrin and Vinogradov [18] shows that the general correlation between tensile strength and endurance limit of metals also holds for a variety of SPD processed conditions. Even though microstructural details are not provided for all fatigue test data in the overview, the different processing conditions indicate that it covers a wide range of HAGB fractions including some precursors to UFG microstructures. Moreover, Ueno et al. [19] have shown that the endurance limit scales with the tensile strength for 316L stainless steel subjected to one and three ECAP passes, yet, these results might not be transferable to the majority of metals due to its low stacking fault energy and resulting nanotwinned structure.

The aim of the present work is a comparison of microstructures and mechanical properties under monotonic and cyclic loading for bcc iron subjected to different levels of plastic strain, with an emphasis on precursors to UFG microstructures generated at imposed plastic strains of 1–2. Strains in this range can also be imposed by conventional cold forming processes, which are usually more economical than SPD processes. Therefore, a single pass ECAP and cold rolling are investigated as well as a combination of a single pass ECAP followed by rolling, as rolling after ECAP has proven to generate good fatigue properties in UFG conditions [1]. These conditions will be compared to a coarse grained (strain free) reference condition and a UFG reference condition from a previous investigation [17].

2. Materials and Methods

Hot rolled square bars of ARMCO® iron (wt % 0.04C, 0.003Si, 0.062Mn, 0.004P, 0.005S, 0.011Cu, 0.022Cr, 0.021Ni, 0.006Mo, 0.004Al, 0.003N, 0.003Sn, balance Fe) were used for the present investigations. Billets for ECAP and cold rolling were machined from the as-received square bars to a size of 20 × 20 × 90 mm^3. ECAP was performed at room temperature using a cold forging lubricant (Beruforge 150, Carl Bechem GmbH, Hagen, Germany) to reduce friction between billet and die walls. The samples were processed by ECAP in a 90° die with sharp outer and inner corners. A feed rate of 0.5 mm/s was used with an applied backpressure of 50 MPa. For this geometry, the equivalent nominal strain per pass amounts to 1.15 [1]. The reference condition with UFG microstructure was generated by five ECAP passes following route B_C (90° clockwise rotation in between passes). Cold rolling was performed on as-received as well as one pass ECAP processed billets using a two high rolling mill. A total rolling reduction of approx. 64% (20 mm down to 7.25 mm height) was induced in 25 rolling passes, which corresponds to an equivalent logarithmic strain of 1.17 assuming ideal plane strain compression.

All mechanical tests were performed parallel to the ECAP extrusion axis or rolling direction of the last processing step. Tensile tests were conducted using round specimens with 15 mm gage length and 3 mm gage diameter. For each condition, three samples were tested at a constant cross-head speed of 15 µm/s that corresponds to an initial strain rate of 10^{-3} s^{-1}. High cycle fatigue tests were performed using hourglass shaped specimens with a minimum diameter of 3.38 mm in a four-point rotating bending test system (stress ratio $R = -1$). The samples were turned from wire cut cylinders using a cooling lubricant. The gage section of the turned samples was ground and polished mechanically followed by pulsed electropolishing to avoid mechanical damage at the surface from the sample preparation. The tests were conducted at 50 Hz with a failure criterion corresponding to a reduction of the initially applied bending moment by 0.15 Nm, which corresponds to a moderate amount of crack propagation. The stress amplitude at the surface was calculated as $\Delta\sigma/2 = 32M/\pi d^3$ with M being the applied bending moment and d being the center diameter after electropolishing, which was measured for each sample using a stereomicroscope.

Microstructural analyses were performed using electron channeling contrast imaging and electron backscatter diffraction (EBSD, AMETEK EDAX, Berwyn, IL, USA) in a scanning electron microscope (SEM, TESCAN, Brno, Czech Republic). The covered area and step size of the EBSD maps was adjusted according to the microstructural length scales of the different conditions. Multiple scans were combined for each condition to improve the statistics for texture analysis. The total covered areas and step sizes are 2500 µm^2 at 30 nm step size for five passes ECAP route B_C, 2.8 mm^2 at 1 µm step size for the as-received condition, and 0.15 mm^2 at 150 nm step size for all the other conditions. Crystallographic textures were calculated from EBSD datasets using the harmonic series expansion method with a series rank of 20 and a Gaussian half width of 5°.

3. Results

3.1. Microstructure

The microstructures before and after processing are compared based on inverse pole figure maps from EBSD analyses that are presented in Figure 1, with quantifications given in Table 1. The HAGB fraction and the total boundary density S_V—i.e., boundary length per unit area—are chosen as microstructural parameters to quantify the refinement. The latter includes all boundaries with a misorientation above 2° and represents a more appropriate measure than the grain size, which is not well defined for heavily cold worked microstructures and strongly depends on thresholds used in the EBSD analysis.

The as-received condition (Figure 1a) exhibits a nearly equiaxed microstructure with no deformation substructures inside the grains and an average grain size (arithmetic mean) of approximately 50 µm. After cold rolling to an equivalent logarithmic strain of 1.17, the microstructure is elongated with a pronounced subgrain structure that is observable as color variations in the inverse pole figure map in Figure 1b. Compared to the as-received condition, the total boundary density has increase by a factor of 30 whereas the HAGB fraction has decreased from 96% down to 19%. Imposing an equivalent nominal strain of 1.15 by ECAP results in a higher total boundary density and larger fraction of HAGBs as compared to the cold rolled condition (Table 1), indicating that simple shear deformation is more effective in terms of structural refinement than plain strain compression. This is also observable in Figure 1c, which shows more regions with deformation induced HAGBs, which are marked as black lines, than Figure 1b. A combination of ECAP and cold rolling leads to another substantial increase in total boundary density and HAGB fraction as compared to either of the two processing steps. Even though the average boundary spacing is in the submicron range and a lot of new HAGBs have been generated (black lines in Figure 1d), the majority of boundaries is still of low angle character (Table 1). Thus, the condition is still a precursor to an UFG microstructure. After five ECAP passes following route B_C (Figure 1e), a UFG microstructure has developed with a

HAGB fraction of 61% and a total boundary density that is two orders of magnitude higher than in the as-received condition.

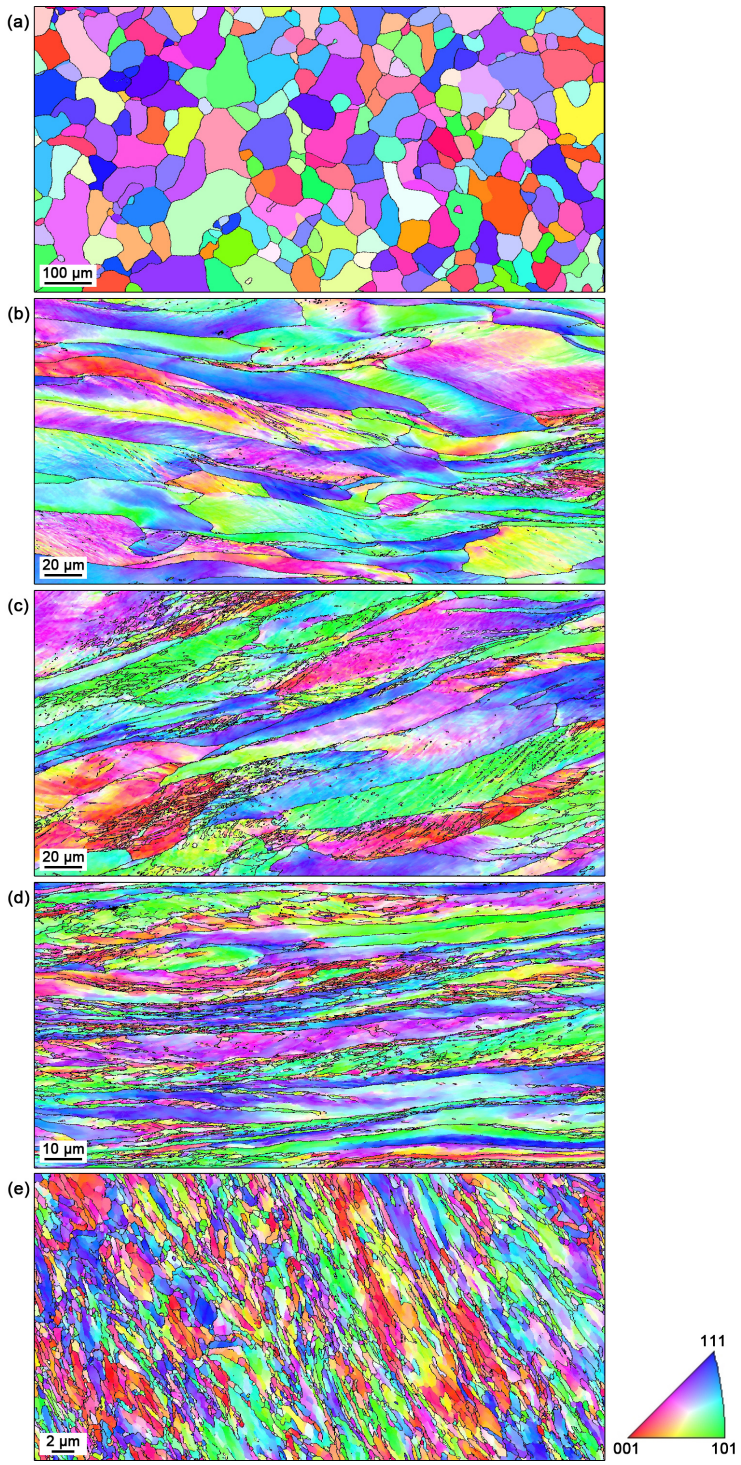

Figure 1. Inverse pole figure maps for ARMCO® iron (**a**) as-received; (**b**) after cold rolling to 64% rolling reduction; (**c**) after one ECAP pass; (**d**) after one ECAP pass followed by cold rolling to 64% rolling reduction; (**e**) after five ECAP passes along route B_C. Black lines indicate high angle grain boundaries (>15° misorientation). Please note the different scale bars.

Table 1. Fraction of high angle grain boundaries (HAGBs), total boundary density (S_V), texture index (TI), average Taylor factor along the tensile axis (M_{tens}), ultimate tensile strength (σ_{UTS}), endurance limit based on 10^7 cycles (σ_f), and fatigue ratio (σ_f/σ_{UTS}) for ARMCO® iron in different processing conditions

Sample Condition	HAGBs [%]	S_V [μm^{-1}]	TI	M_{tens}	σ_{UTS} [MPa]	σ_f [MPa]	σ_f/σ_{UTS}
As-Received	96	0.05	1.3	3.05	297	225	0.76
64% Cold Rolled	19	1.55	3.0	3.21	624	350	0.56
1 × ECAP	25	2.09	2.1	3.03	595	335	0.56
1 × ECAP + 64% Cold Rolled	37	3.21	3.4	3.19	706	395	0.56
5 × ECAP Route B_C	61	6.32	2.5	2.97	853	425	0.50

The effect of cyclic loading on the microstructure is investigated qualitatively in cross-sections of fatigue tested samples. Comparisons of the microstructures at the surface of the smallest cross-section (largest stress amplitude) and near the center (neutral fiber) of fatigue tested specimens shows only localized coarsening at the surface of deformed conditions, i.e., cold rolled and ECAP processed samples. This is exemplarily shown in Figure 2 for a sample subjected to one ECAP pass followed by cold rolling. Growth of the grain or subgrain structure is only observable within a few microns from a fatigue crack. In some cases, there is also a zone with a clearer ECCI contrast next to the coarsened region observable, as can be seen in Figure 2b. This indicates a reduced dislocation density, which has also been observed in TEM investigations on fatigue tested UFG metals by other groups [15,16]. Further details on the damage mechanisms of the UFG reference condition are given in [17].

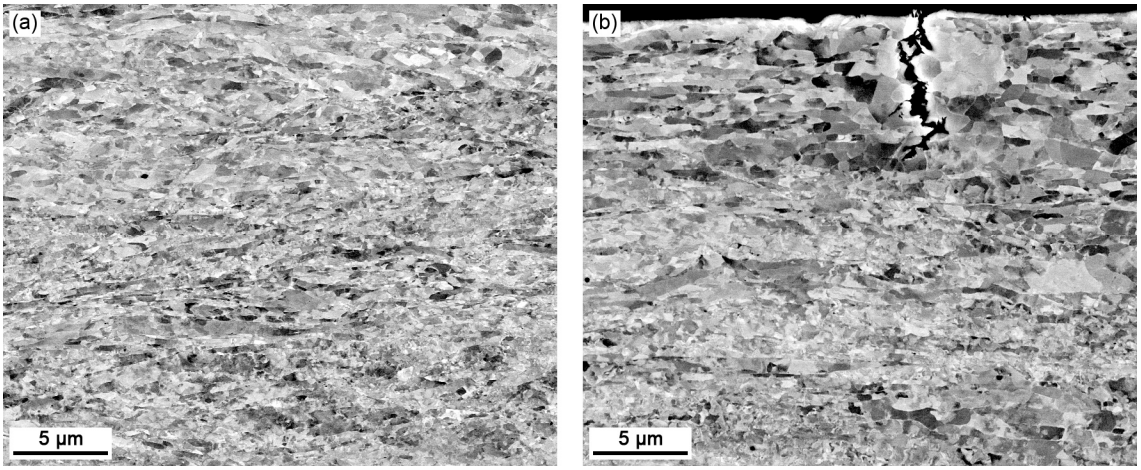

Figure 2. Electron channeling contrast images of fatigue tested ARMCO® iron ($N_f = 7 \times 10^5$) processed by one ECAP pass followed by 64% cold rolling (**a**) at the neutral fiber of the rotating bending specimen and (**b**) at the surface of the smallest cross-section.

Processing routes with different modes of deformation, such as ECAP and cold rolling, result in different crystallographic textures and can cause an anisotropy of mechanical properties. To evaluate the potential effect of anisotropy on the mechanical properties, crystallographic textures are analyzed based on multiple EBSD measurements from each condition. The (110) pole figures in Figure 3 show a nearly random texture for the coarse grained reference condition which develops into a typical simple shear or rolling texture after one ECAP pass or after cold rolling, respectively [20]. The textures after one and five ECAP passes are qualitatively similar with slightly higher intensities after five passes. The textures after 64% rolling reduction with and without a prior ECAP pass are also similar, which shows that the imposed strain during cold rolling was sufficiently high to transform the simple shear texture after ECAP into a rolling texture. In general, the texture intensities after cold rolling are stronger than after ECAP, which is reflected by a higher texture index (Table 1).

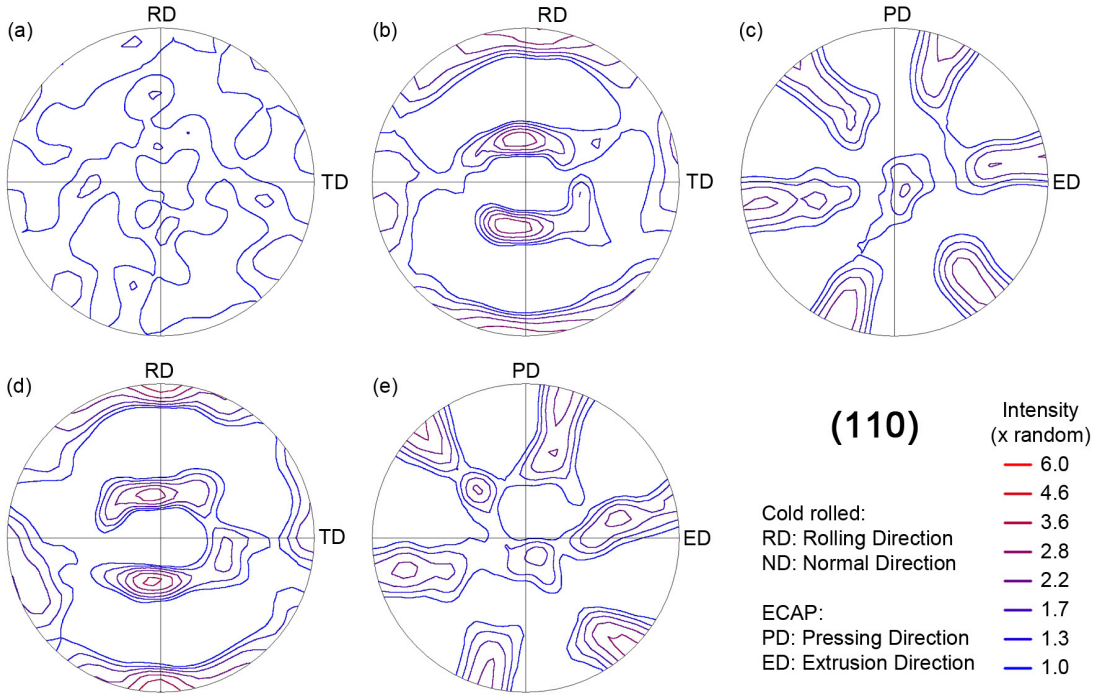

Figure 3. (110) pole figure maps for ARMCO® iron (**a**) as-received; (**b**) after cold rolling to 64% rolling reduction; (**c**) after one ECAP pass; (**d**) after one ECAP pass followed by cold rolling to 64% rolling reduction; (**e**) after five ECAP passes along route B_C.

3.2. Mechanical Properties

The engineering stress–strain curves of the investigated conditions (Figure 4) exhibit the typical behavior of metals subjected to SPD processes. The yield and tensile strength increase with imposed strain whereas the uniform elongation falls below 1%. Yet, all tested conditions still show a ductile material behavior with a pronounced post necking elongation. The curves for cold rolling with a logarithmic strain of 1.17 (red) and a single ECAP pass with a nominal strain of 1.15 (blue) are very similar, in spite of the difference between nominal and logarithmic equivalent strains. Both processes result in an increase in yield strength by more than 100% as compared to the as-received condition. The combination of one ECAP pass and subsequent cold rolling (green curve) results in a further increase in yield strength by about 100 MPa, i.e., approximately 17%, as compared to just either of these processes. The UFG reference condition subjected to five ECAP passes along route B_C exhibits the highest yield strength among all tested conditions with an increase of 45% as compared to the first ECAP pass.

The *S*–*N* curves in Figure 5 provide a comparison of the fatigue life for the investigated conditions in the high cycle fatigue regime under four-point rotating bending (stress ratio $R = -1$). It has to be considered that the testing method results in an overestimation of stress amplitudes if the stress at the surface exceeds the yield strength of the material. This is due to the fact that the stress calculation based on the bending moment assumes a linear elastic behavior. However, this does only affect the as-received condition below 10^6 cycles, whereas the peak stresses of all the other conditions are well below the macroscopic yield point. The endurance limit of 225 MPa for the as-received state (50 µm grain size) is close to literature values of approx. 210 MPa that were reported for 100 µm grain size [21]. The *S*–*N* curves of all the deformed conditions show a substantially higher fatigue strength than the as-received condition, with an increase of at least 50% in stress amplitude for a given number of cycles to failure. The variation of the stress amplitudes in between the deformed states does not exceed 30% and seems to converge towards lower numbers of cycles to failure, i.e., towards higher fatigue loads. With regard to the 10^7 cycles endurance limits, the lowest values among the deformed

conditions are found for the lowest imposed strains, i.e., after a single pass of ECAP (σ_f~335 MPa) and cold rolling with (σ_f~350 MPa). The combination of both processes does result in an increase in σ_f to ~395 MPa, which is already close to the value after five ECAP passes of ~425 MPa (Table 1). Hence, the variation in high cycle fatigue strength between the UFG reference condition and precursors to UFG microstructures is not very pronounced, especially when considering the combination of ECAP and rolling.

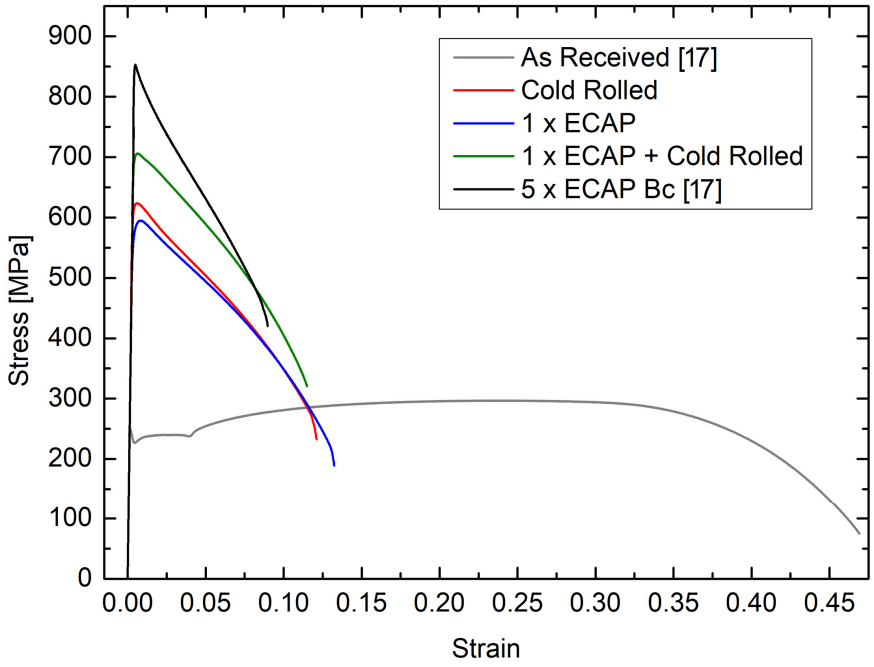

Figure 4. Engineering stress–strain curves for different processing conditions of ARMCO® iron.

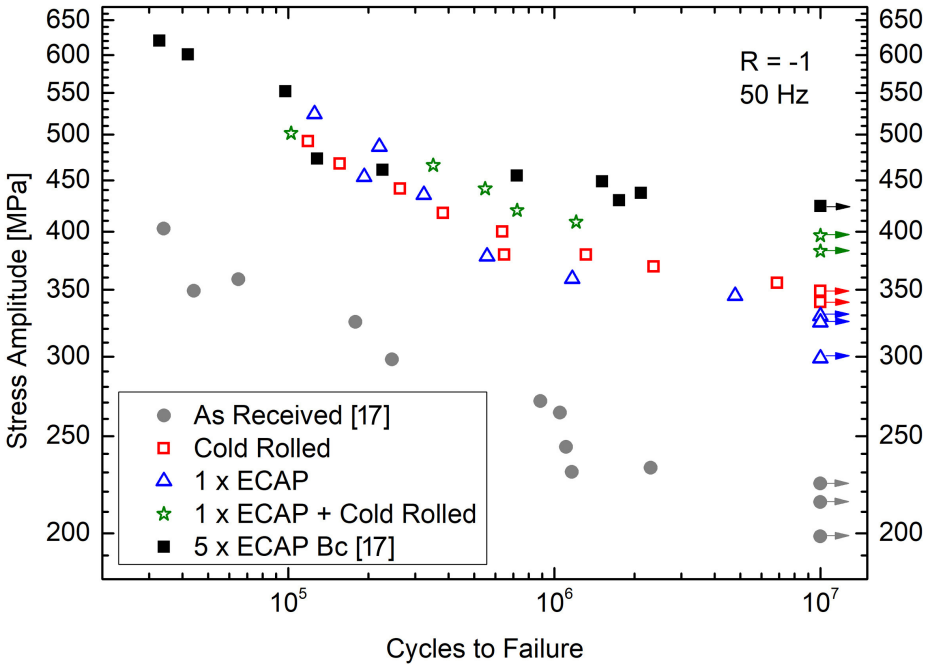

Figure 5. *S–N* diagrams for ARMCO® iron in different processing conditions under four-point rotating bending loads.

4. Discussion

The results above provide a comprehensive picture of the microstructures and corresponding mechanical properties of ARMCO® iron after large and severe plastic strain using either ECAP, cold rolling or a combination of both processes. In the following section, these results will be discussed with respect to the relation between tensile strength, endurance limit and HAGB fraction, as well as in terms of the fatigue strength to processing effort ratio.

The ratios between the endurance limit σ_f and the ultimate tensile strength σ_{UTS} for the tested conditions (Table 1) show that a general ratio of approximately 50%, which is typically reported for steels in literature [22], does hold for the deformed conditions but not for the as-received state. The high ratio of this condition might be related to the effect of interstitial atoms, given that this condition is the only one with an upper and lower yield point followed by a Lüders strain. It is known from literature that the presence of a Lüders strain can affect the endurance limit [21]. Another aspect that could play a role is the change in strain rate sensitivity of the material, which generally decreases with decreasing grain size or increasing work hardening for bcc metals [23]. A higher sensitivity in the as-received condition as compared to the deformed conditions can affect the relation between monotonic and cyclic properties if the strain rates vary substantially. Yet, this contribution is difficult to assess for macroscopically elastic cyclic loading and plasticity being confined to slip bands with unknown local strain rates. However, plotting the endurance limit as a function of the tensile strength (Figure 6) shows that there is a proportionality between both parameters for all investigated conditions but with an offset of 117 MPa. The as-received, cold rolled, and one pass ECAP conditions show a perfectly linear relation, whereas the ECAP plus cold rolled condition lies above the linear regression. This confirms the hypothesis that a combination of ECAP and subsequent rolling can lead to an excellent high cycle fatigue strength, even for precursors to UFG microstructures, which consists of a majority of LAGBs.

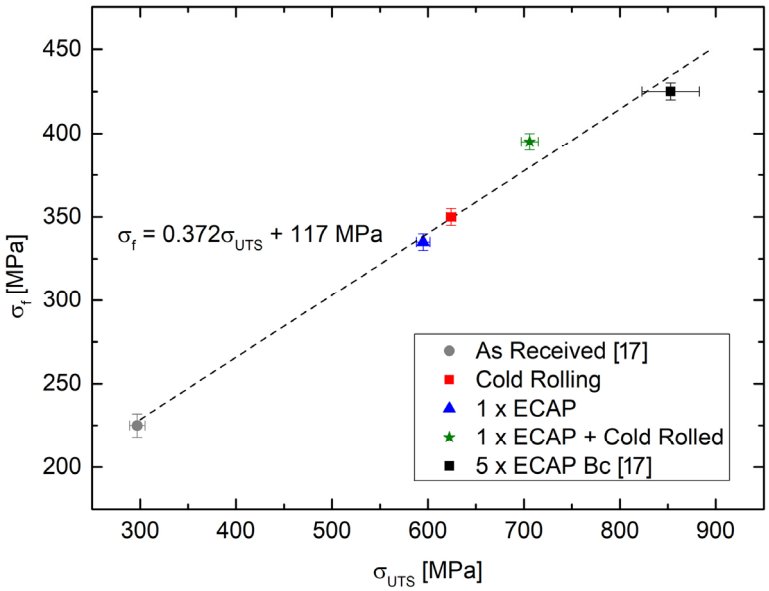

Figure 6. Endurance limit (σ_f) for rotating bending fatigue as a function of ultimate tensile strength (σ_{UTS}) for ARMCO® iron in different processing conditions. The error bars indicate the uncertainty in the determination of σ_f and the scatter range for σ_{UTS} from tensile tests.

The increase in strength in the tensile tests can be attributed to the formation of subgrain structures and new high angle boundaries, both of which contribute to the observed increase in boundary density (Table 1). Yet, the relation between total boundary density and yield or tensile strength is only qualitative but not quantitative. There are approaches in literature that divide the total boundary density into high angle and low angle fractions to separate the strengthening contributions

into a Hall–Petch and a Taylor hardening component [24]. Yet, this does not hold for the present results when considering that the boundary density and HAGB fraction after one ECAP pass is significantly higher than after cold rolling, whereas the strength of the ECAP condition is actually slightly lower. One explanation could be that the heterogeneity of deformation, which controls the formation of geometrically necessary boundaries, is higher during ECAP as compared to cold rolling, thus promoting the formation of subgrain structures. Another factor that needs to be considered is the anisotropy of mechanical properties that stems from the differences between rolling and simple shear textures. To evaluate the role of plastic anisotropy on tensile properties, the average Taylor factor for uniaxial loading along the tensile axis M_{tens} was calculated from EBSD datasets for each condition considering only {110} <111> slip systems (Table 1). Even though this analysis is far too simple for a quantitative estimate, it can provide trends towards higher or lower strength values as compared to a random texture. The conditions processed by one and five ECAP passes show a lower Taylor factor than the 3.05 for the as-received state with nearly random texture, even though this effect is marginal after one ECAP pass with a Taylor factor of 3.03 as compared to 2.97 after five passes. In contrast, both conditions with a rolling texture show a higher Taylor factor along the tensile axis of approx. 3.2 after cold rolling as well as after one ECAP pass followed by cold rolling. Consequently, it is not surprising that the strength of the cold rolled condition along the rolling direction is higher than what might be expected based on the total boundary density. The influence of texture on the fatigue properties is difficult to assess, as this would require tests in different directions that are complicated by sample size limitations. A certain effect is likely though, considering that crystallographic texture often affects yield strength and high cycle fatigue strength in a similar direction, yet the extent varies between materials [25,26].

Regarding the role of HAGBs for the high cycle fatigue properties, it is obvious that there is no correlation between the HAGB fraction and the endurance limit. This is supported by the observation that cyclic coarsening occurs only locally near fatigue cracks even for precursor states. In fact, the UFG reference condition subjected to five ECAP passes, which should exhibit a higher cyclic stability than the precursor states, shows the lowest fatigue ratio among all tested conditions (Table 1). It even falls slightly below the linear regression in Figure 6 (black square), though this could also be attributed to the large scatter band of σ_{UTS} for this condition, as well as anisotropy effects [17]. Even though a cyclic stability is to be expected for UFG microstructures under stress controlled high cycle fatigue tests [15,16], this also seems to hold for their precursor states. Hence, a large fraction of LAGBs may be detrimental for the low cycle fatigue behavior as shown by Niendorf et al. [13,14] but it is not a crucial aspect for the stress controlled high cycle fatigue performance.

Improving the mechanical properties of SPD processed materials and understanding the underlying mechanisms is without doubt highly relevant from a materials science perspective. Yet, even outstanding properties do not necessarily go along with a high potential for commercial applications, as the processing might be too costly to be justified. Against this backdrop, it appears that the ratio of mechanical properties to processing effort is rather unfavorable for the UFG reference condition subjected to five ECAP passes, in spite its high monotonic and cyclic strength. In comparison to a single ECAP pass or 64% rolling reduction, the endurance limit increases by just about 25%, at the cost of a processing effort that is several times higher. One might argue that there are ECAP related processes with continuous feeding options which are more economical than the discontinuous approach used in this work, such as ECAP conform [27] or equal-channel angular swaging (ECAS) [28]. However, they do have other limitations in terms of maximum cross-sections in case of ECAP conform or in terms of processing routes and channel angles in case of ECAS. Considering that discontinuous ECAP can be scaled up to large dimensions [29] but the effort is nearly proportional to the number of passes, a combination of a single ECAP pass and subsequent cold forming such as rolling, swaging, or extrusion is a promising approach, especially for large sample dimensions. Even though similar mechanical properties could probably be achieved without ECAP by cold rolling to logarithmic strains of 2–3, this may not always be a viable option. Considering that the dimensions of the sample

or product often limit the amount of cold working due to geometrical constraints, a combination of strain accumulation without change in dimensions (e.g., ECAP) and with dimensional changes (e.g., cold rolling or drawing) appears reasonable. The present results show that such a combination can achieve more than 90% of the endurance limit of a true UFG condition after multiple ECAP passes at only a fraction of the processing effort.

5. Conclusions

The microstructure and mechanical properties of ARMCO® iron have been investigated for different processing conditions including a single ECAP pass, cold rolling, and ECAP followed by cold rolling. These conditions can be considered as precursors to UFG microstructures and have been compared to a UFG reference condition processed by five ECAP passes along route B_C as well as a strain free condition reported in [17]. The main conclusions can be summarized as follows:

1. A single ECAP pass and cold rolling with 64% rolling reduction result in different HAGB fractions and total boundary densities but similar mechanical properties, which indicates a different heterogeneity of deformation in both processes.
2. The crystallographic textures are governed by the last processing step, which leads to either rolling or simple shear textures, with higher texture intensities in case of rolled conditions. A Taylor factor analysis shows higher values along the tensile and fatigue testing direction for conditions with rolling textures as compared to those with shear textures, thus indicating that the mechanical properties are most likely affected by plastic anisotropy.
3. There is a linear relation between endurance limit and tensile strength for all investigated conditions, yet, with a positive endurance limit offset. Hence, the ratio of endurance limit and tensile strength decreases with increasing tensile strength showing the highest value for the strain free condition and the lowest value for the UFG reference condition, with intermediate values for the precursors to UFG microstructures.
4. A large fraction of LAGBs, as is found in the precursor states, does not negatively affect the high cycle fatigue behavior, as there is no correlation between the HAGB fraction and the high cycle fatigue properties of the tested conditions.
5. A combination of a single ECAP pass followed by cold rolling is a good compromise in terms of processing effort and mechanical properties as it achieves more than 90% of the endurance limit of the UFG reference condition, which emphasizes the application potential for precursors to UFG microstructures.

Acknowledgments: The author acknowledges support by the German Research Foundation (DFG) under the grant number BR 4614/1-1 and the Open Access Publishing Fund of Technische Universität Darmstadt. The author also acknowledges Petra Neuhäusel, Claudia Wasmund, and Mehmet Baran Bas for the preparation of the fatigue test samples.

Conflicts of Interest: The author declares no conflict of interest.

References

1. Valiev, R.Z.; Langdon, T.G. Principles of equal-channel angular pressing as a processing tool for grain refinement. *Prog. Mater. Sci.* **2006**, *51*, 881–981. [CrossRef]
2. Zhilyaev, A.P.; Langdon, T.G. Using high-pressure torsion for metal processing: Fundamentals and applications. *Prog. Mater. Sci.* **2008**, *53*, 893–979. [CrossRef]
3. Saito, Y.M.; Utsunomiya, H.; Tsuji, N.; Sakai, T. Novel ultra-high straining process for bulk materials—Development of the accumulative roll-bonding (ARB) process. *Acta Mater.* **1999**, *47*, 579–583. [CrossRef]

4. Valiev, R.Z.; Estrin, Y.; Horita, Z.; Langdon, T.G.; Zehetbauer, M.J.; Zhu, Y.T. Producing bulk ultrafine-grained materials by severe plastic deformation. *JOM* **2006**, *58*, 33–39. [CrossRef]
5. Estrin, Y.; Vinogradov, A. Extreme grain refinement by severe plastic deformation: A wealth of challenging science. *Acta Mater.* **2013**, *61*, 782–817. [CrossRef]
6. Kawasaki, M.; Horita, Z.; Langdon, T.G. Microstructural evolution in high purity aluminum processed by ECAP. *Mater. Sci. Eng. A* **2009**, *524*, 143–150. [CrossRef]
7. Xu, C.; Furukawa, M.; Horita, Z.; Langdon, T.G. The evolution of homogeneity and grain refinement during equal-channel angular pressing: A model for grain refinement in ECAP. *Mater. Sci. Eng. A* **2005**, *398*, 66–76. [CrossRef]
8. Kim, H.S.; Ryu, W.S.; Janecek, M.; Baik, S.C.; Estrin, Y. Effect of Equal Channel Angular Pressing on Microstructure and Mechanical Properties of IF Steel. *Adv. Eng. Mater.* **2005**, *7*, 43–46. [CrossRef]
9. Dalla Torre, F.; Lapovok, R.; Sandlin, J.; Thompson, P.F.; Davies, C.H.J.; Pereloma, E.V. Microstructures and properties of copper processed by equal channel angular extrusion for 1–16 passes. *Acta Mater.* **2004**, *52*, 4819–4832. [CrossRef]
10. Han, B.Q.; Mohamed, F.A.; Lavernia, E.J. Mechanical Properties of Iron Processed by Severe Plastic Deformation. *Metall. Mater. Trans. A* **2003**, *34*, 71–83. [CrossRef]
11. Fukuda, Y.; Oh-ishi, K.; Horita, Z.; Langdon, T.G. Processing of a low-carbon steel by equal-channel angular pressing. *Acta Mater.* **2002**, *50*, 1359–1368. [CrossRef]
12. Höppel, H.W.; Mughrabi, H.; Vinogradov, A. Fatigue properties of bulk nanostructured materials. In *Bulk Nanostructured Materials*; Zehetbauer, M.J., Zhu, Y.T., Eds.; Wiley-VCH: Weinheim, Germany, 2009; pp. 481–500, ISBN 9783527315246.
13. Niendorf, T.; Canadinc, D.; Maier, H.J.; Karaman, I. On the Microstructural stability of ultrafine-grained interstitial-free steel under cyclic loading. *Metall. Trans. A* **2007**, *38*, 1946–1955. [CrossRef]
14. Niendorf, T.; Canadinc, D.; Maier, H.J.; Karaman, I.; Sutter, S.G. On the fatigue behavior of ultrafine-grained interstitial-free steel. *Int. J. Mater. Res.* **2006**, *97*, 1328–1336. [CrossRef]
15. Kunz, L.; Lukáš, P.; Pantělejev, L.; Man, O. Stability of ultrafine-grained structure of copper under fatigue loading. *Procedia Eng.* **2011**, *10*, 201–206. [CrossRef]
16. Kunz, L.; Lukáš, P.; Svoboda, M. Fatigue strength, microstructural stability and strain localization in ultrafine-grained copper. *Mater. Sci. Eng. A* **2006**, *424*, 97–104. [CrossRef]
17. Bruder, E.; Gangaraju, C.; Lapovok, R. Influence of equal channel angular pressing on high cycle fatigue behavior of ultrafine-grained iron: Role of anisotropy. *Mater. Sci. Eng. A* **2018**, *711*, 650–658. [CrossRef]
18. Estrin, Y.; Vinogradov, A. Fatigue behaviour of light alloys with ultrafine grain structure produced by severe plastic deformation: An overview. *Int. J. Fatigue* **2010**, *32*, 898–907. [CrossRef]
19. Ueno, H.; Kakihata, K.; Kaneko, Y.; Hashimoto, S.; Vinogradov, A. Enhanced fatigue properties of nanostructured austenitic SUS 316L stainless steel. *Acta Mater.* **2011**, *59*, 7060–7069. [CrossRef]
20. Kocks, U.F.; Tomé, C.N.; Wenk, H.-R. *Texture and Anisotropy*; Cambridge University Press: Cambridge, UK, 1998; pp. 178–238, ISBN 0521465168.
21. Phillips, W.L.; Armstrong, R.W. The influence of specimen size, polycrystal grain size, and yield point behaviour on the fatigue strength of low-carbon steel. *J. Mech. Phys. Solids* **1969**, *17*, 265–270. [CrossRef]
22. Dieter, G.E. *Mechanical Metallurgy*, 3rd ed.; McGraw-Hill Publishing: New York, NY, USA, 1986; pp. 376–431, ISBN 0070168938.
23. We, Q.; Cheng, S.; Ramesh, K.T.; Ma, E. Effect of nanocrystalline and ultrafine grain sizes on the strain rate sensitivity and activation volume: Fcc versus bcc metals. *Mater. Sci. Eng. A* **2004**, *381*, 71–79. [CrossRef]
24. Hansen, N. Hall-Petch relation and boundary strengthening. *Scr. Mater.* **2004**, *51*, 801–806. [CrossRef]
25. Bowen, A.W. The effect of testing direction on the fatigue and tensile properties of a Ti–6Al–4V bar. In *Proceedings of the Second World Conference on Titanium Science and Technology;* Jaffee, R.I., Burte, H.M., Eds.; Plenum Press: New York, NY, USA, 1973; pp. 1271–1281.
26. Mateo, A.; Llanes, L.; Akdut, N.; Anglada, M. High cycle fatigue behaviour of a standard duplex stainless steel plate and bar. *Mater. Sci. Eng. A* **2001**, *319–321*, 516–520. [CrossRef]
27. Raab, G.J.; Valiev, R.Z.; Lowe, T.C.; Zhu, Y.T. Continuous processing of ultrafine grained Al by ECAP-Conform. *Mater. Sci. Eng. A* **2004**, *382*, 30–34. [CrossRef]

28. Bruder, E.; Görtan, M.O.; Groche, P.; Müller, C. Severe plastic deformation by equal channel angular swaging. *Mater. Sci. Forum* **2011**, *667–669*, 103–107. [CrossRef]
29. Frint, S.; Hockauf, M.; Frint, P.; Wagner, M.F.X. Scaling up Segal's principle of Equal-Channel Angular Pressing. *Mater. Des.* **2016**, *97*, 502–511. [CrossRef]